Particle-in-cell numerical simulations of a two-dimensional model of cylindrical Hall thrusters with permanent magnets

IEPC-2017-282

Presented at the 35th International Electric Propulsion Conference
Georgia Institute of Technology – Atlanta, Georgia – USA
October 8–12, 2017

Rodrigo A. Miranda*
UnB-Gama Campus, and Plasma Physics Laboratory,
University of Brasília (UnB), Brasília DF 70910-900, Brazil

Alexandre A. Martins†
Plasma Physics Laboratory,
University of Brasília (UnB), Brasília DF 70910-900, Brazil

and

José L. Ferreira‡
Plasma Physics Laboratory,
University of Brasília (UnB), Brasília DF 70910-900, Brazil

Abstract: The cylindrical Hall thruster (CHT) is a propulsion device that offers high propellant utilization and performance at smaller dimensions and lower power levels than traditional Hall thrusters. In this paper we present first results of a numerical model of a CHT. This model solves particle and field dynamics self-consistently using a particle-in-cell approach. We describe a number of techniques applied to reduce the execution time of the numerical simulations. The specific impulse and thrust computed from our simulations are in agreement with laboratory experiments. This simplified model will allow for a detailed analysis of different thruster operational parameters and obtain an optimal configuration to be implemented at the Plasma Physics Laboratory at the University of Brasília.

*Professor, Aerospace Engineering, rmiracer@unb.br.
†Post-doctoral researcher, Institute of Physics
‡Professor, Institute of Physics

Nomenclature

Δt = time step
ϕ = electric potential
ζ = self-similar scaling law
$\mathbf{B}$ = magnetic field
$\mathbf{E}$ = electric field
g = acceleration of gravity
I = current
I_{sp} = specific impulse
m = mass flow rate
m_i = ion mass flow rate
n = particle number density
N_p = number of particles in a superparticle
r = radial direction
T = thrust
v_i = ion velocity
z = axial direction

I. Introduction

Hall thrusters (HTs) are electromagnetic propulsion devices that apply a cross-field discharge in an annular channel to generate a plasma.[1] A radial magnetic field is responsible for electron trapping in the channel, forming the electron Hall current and a virtual cathode that helps ionize the neutral gas. An electric field is applied in the axial direction, between the anode and the virtual cathode, and is responsible for ion acceleration. Therefore, the strength of the magnetic field must be chosen to keep only the ions unmagnetized. HTs can achieve higher thrust levels compared to ion thrusters, and are simpler to construct. However, their scalability to smaller dimensions compatible for micro and nano-satellites present several challenges. For example, since the surface-to volume ratio in the annular channel increases, the collisions between particles and walls increase as well, leading to heating and higher erosion rates. Moreover, the reduced thruster dimensions makes the magnetic circuit difficult to maintain. The scaling down of HTs to various power levels has been the subject of several studies.[2–5]

The cylindrical Hall thruster (CHT) is an alternative concept first developed at the Princeton Plasma Physics Laboratory.[6] It consists of a cylindrical region and a short annular channel with variable depth, and presents an increased volume-to-surface ratio in comparison to compact HTs, potentially reducing wall erosion. The CHT presents higher propellant utilization and comparable performance with conventional HTs.[7] The magnetic field in this thruster can be set by using electromagnets or permanent magnets.[8]

The CHT has been characterized through laboratory experiments[6,8–10] and numerical simulations.[7,11,12] Several strategies have been applied to model the CHT numerically. For example, Smirnov et al.[11] used particle-tracing to study the cross-field diffusion of electrons in a typical magnetic field configuration of a two-dimensional (2D) model of a CHT. They showed that the electrons are most concentrated near the annular region of the CHT. Garrigues et al.[7] applied an hybrid model consisting of a fluid description of electrons and particle description of neutrals and ions to a 2D model of a CHT. Their results show that the ionization occurs in the annular region, and that the doubly charged ions play an important role on the level of propellant efficiency. A three-dimensional particle-in-cell (PIC) model of a CHT was proposed and studied by Matyash et al.[12] They were able to reproduce asymmetric features of the Hall current known as "spokes" commonly observed in laboratory experiments,[13] and found that the depletion of neutral gas leading to azimuthal asymmetry of the discharge is a possible cause of these features.

The Plasma Physics Laboratory at the University of Brasília has been developing Hall thrusters with permanent magnets for the Brazilian Space Program since 2004.[14] The team is currently investigating alternatives to conventional HTs, such as the CHT. The reduced dimensions of the CHT operating at lower power levels makes it an interesting option of electric propulsion device for future Brazilian space missions. A numerical model is in development for testing operational parameters and performance for a future CHT prototype to be constructed at the laboratory.

In this paper we present the first results of a simplified 2D model of a CHT using PIC code. This paper is organized as follows. Section II introduces the numerical model of a CHT. Our numerical results are presented in Section III. The conclusions are indicated in Section IV.

II. Numerical model

Following previous works[7,9,11] we adopt cylindrical coordinates and neglect variations in the azimuthal direction to define a two-dimensional simulation domain representing the upper-half of a cross-section of the CHT. The 2D axisymmetric model allows to reduce the time needed to perform computations. The geometry of the simulation domain, including particle sources and boundary conditions of particles and fields, is summarized in Figure 1. We dispose the axial direction z as the horizontal axis, and the radial direction r as the vertical direction. The size of the simulation domain is $[-16, 30] \times [0, 30]$ mm.

A. Field solver

The thruster's magnetic field $\mathbf{B}$ is assumed to be static. The magnetic field generated by permanent magnet rings is modelled and computed using the Comsol software.[15] The resulting vector field is depicted in Figure 2(a). Fig. 2(b) shows the modulus of the magnetic field $|\mathbf{B}|$ as a function of the axial distance, at $r = 13.8$ mm and at $r = 20$ mm, which are the position of the inner dielectric surface at the core and the position of the outer dielectric surface, respectively. The $|\mathbf{B}|$ profiles are in agreement with laboratory experiments.[6,10]

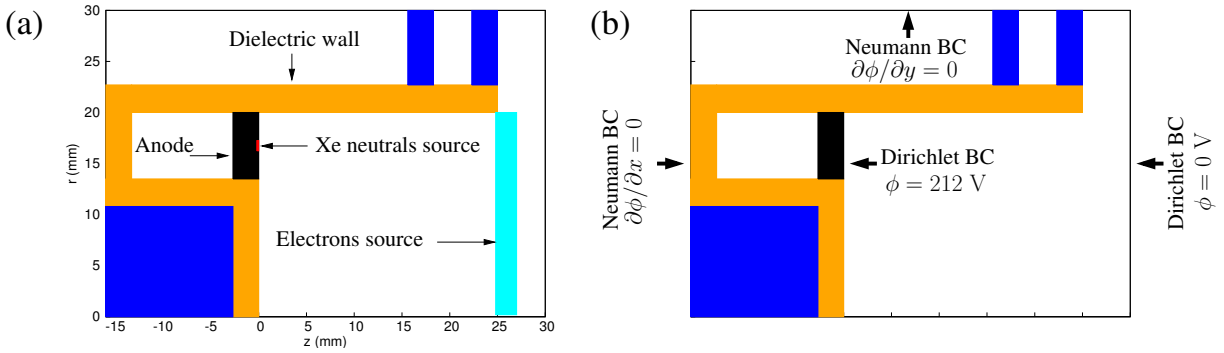

Figure 1. The simulation domain representing the upper-half cross-section of a cylindrical Hall thruster, showing (a) particle sources and boundaries, and (b) boundary conditions of the electric potential ϕ. Blue represents the structure supporting the dielectric wall.

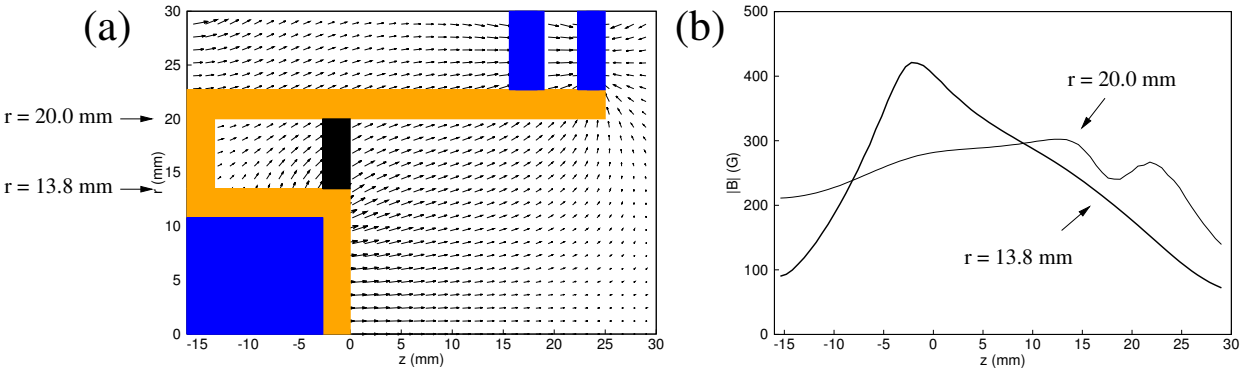

Figure 2. (a) The magnetic vector field $\mathbf{B}(z, r)$ in the simulation domain. (b) The modulus of the magnetic field, $|\mathbf{B}|$, as a function of the axial distance z, at $r = 13.8$ mm (thick line), and $r = 20$ mm (thin line).

The electric potential ϕ is solved using a self-consistent algorithm described in the next section. We set different boundary conditions for the electric potential ϕ as follows. Neumann boundary conditions are set at the $z = -16$ mm and $r = 30$ mm boundaries. At $z = 30$ mm we set a Dirichlet boundary condition with $\phi = 0$ V. The anode is represented by a region in which $\phi = 212$ V using Dirichlet boundary conditions. These boundary conditions are depicted in Fig. 1(b).

B. Particle solver

We model charged and neutral particles using a PIC description. In this approach, the positions and velocities of charged particles (i.e., electrons and xenon ions) are computed from the equations of motion due to the presence of electric and magnetic fields. The charge density is then discretized to a spatial grid by a weighting process, which allows to solve the Poisson equation to obtain new values of the electric potential and the electric field. These fields are then inserted into the equations of motion of the particles, and the cycle is restarted. Particle simulations are performed using the VSim software.[16] The fields are solved in a spatial grid of size 150×255.

Representing all plasma particles in the simulations of a CHT renders the computational effort practically impossible to reach. A common approach to reduce the computation time in PIC simulations is to simulate superparticles, which are particles that represent a "cloud" or a group of electrons or ions. The position of the superparticle is given by the center of mass of the cloud, and its velocity is given by the mean velocity of the cloud.[17] Therefore, the number of particles present in the simulation is reduced as well as the execution time. We use the superparticle approach to represent electrons, Xe^+ and xenon neutrals (Xe). Neutral superparticles represent 10^7 real Xe particles, whereas electrons and Xe ions superparticles represent 10^5 particles. In the following we will refer to the superparticles as simply "particles".

We model Xe neutrals using superparticles with no charge. In laboratory experiments, the xenon gas is injected through small holes in the CHT anode. To mimic this, the neutral particles enter the simulation domain through a narrow region centered in front of the anode (see Fig. 1(a)). Their initial velocity is taken from a Maxwellian distribution with temperature of 560 K, and the flow rate is set to 4 sccm. Neutral particles that hit the dielectric and anode walls are reflected with a velocity taken from a thermal distribution. Particles that leave the simulation domain are removed.

Electrons are inserted in the simulation through a narrow region located in front of of the exit region as shown in Fig. 1(b). Trying to represent a cathode as the source of electrons would break the cylindrical symmetry of our model. For this reason we simplify the geometry and insert the electrons near the exit region of the CHT with an initial velocity taken from a Maxwellian distribution with temperature of 10 eV. This approach has been used in previous simulations of CHTs.[9,11] Electrons leaving the simulation domain are removed.

C. Particle interactions

The interaction between electrons and Xe neutrals are solved by the VSim software using a MonteCarlo collision (MCC) technique. We implement (Xe, e^-) ionization collisions, (Xe, e^-) elastic scattering, (Xe, e^-) excitation collisions, (Xe, Xe^+) elastic scattering, and (Xe, Xe^+) momentum exchange. When an ionization collision occurs, ions and secondary electrons are created at the position of the incident electron. The energy of the created ion is determined from the temperature of the corresponding neutral particle. The energy of the incident electron decreases due to the ionization threshold energy and the energy of the secondary electron.

D. Scaling laws

In order to speed up the execution of the PIC code further, we apply a self-similar scaling ζ following Taccogna et al.[18] This scaling of the CHT geometry is applied to reduce the channel dimensions linearly while at the same time keeping the main plasma parameters constant. A set of scaling laws is applied to the main variables such as the magnetic field, the electric field, and the mass flow rate. A summary of the scaling laws applied is given in Table 1. The simulation execution time is then reduced, and the original system can be recovered by applying the inverse scaling law. Here we use $\zeta = 0.1$.

Parameter	Scaling law
Length (axial direction)	$z^* = \zeta z$
Length (radial direction)	$r^* = \zeta r$
Electric potential	$\phi^* = \phi$
Magnetic field	$\mathbf{B}^* = \zeta^{-1}\mathbf{B}$
Mass flow rate	$\dot{m}^* = \zeta \dot{m}$
Current	$I^* = \zeta I$
Electric field	$\mathbf{E}^* = \zeta^{-1}\mathbf{E}$
Particle number density	$n^* = \zeta^{-1} n$
Temperature	$T^* = T$

Table 1. The scaling laws applied. An asterisk indicates the scaled variable.

III. Simulation results

We start our simulations by setting the electron source disabled and the Xe source enabled. By doing so, we allow the Xe particles to enter the simulation domain and fill the annular and cylindrical regions. Since the equations of fields and charged particle motion are not solved in this initial stage, the time step is set to $\Delta t = 10^{-8}$ s, which is larger than the time step needed in the presence of charged particles. Fig. 3(a) shows the time series of the Xe neutral density averaged in the region given by $0 < z < 25$ mm and $0 < r < 20$ mm, i.e., the cylindrical region. The average Xe density quickly reaches a steady state. Fig. 3(b) shows a snapshot of the resulting Xe neutral density at $t = 0.01$ s. There is a maximum of neutral Xe density at the source region in front of the anode, and a maximum along the z axis due to converged flux near the cylindrical axis of symmetry.

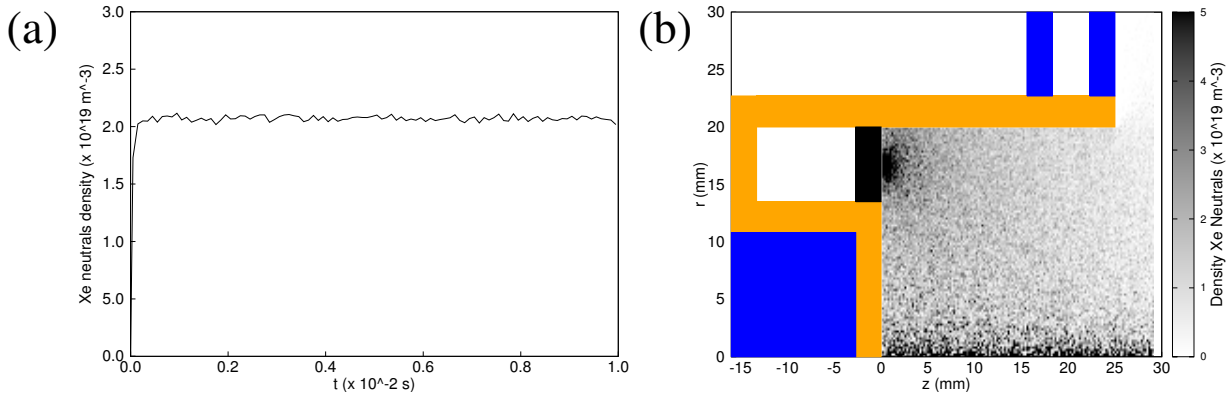

Figure 3. (a) Time series of the average of the Xe neutral density, represented by the gray color. (b) The Xe neutral density at $t = 0.01$ s.

After $t = t_0 = 0.01$ s electrons are introduced by enabling the electron source (see Fig. 1(a)). The time step is reduced to $\Delta t = 10^{-12}$ s to account for the plasma time scales such as the electron plasma frequency. In the following we refer to the simulation time as the time after t_0, i.e., $t - t_0$. Fig. 4(a) shows the electron density at $t = 6.75 \times 10^{-7}$ s. The electrons move toward the anode, and are confined near the center of the cylindrical region due to a combined effect of the electric potential and the magnetic field gradient. The confinement of electrons is clearly seen as a maximum of the electron density in Fig. 4(a).

The electrons ionize the neutral gas producing Xenon ions. Fig. 4(b) shows the density of Xe^+ at $t = 6.75 \times 10^{-7}$ s. Since the ions are unmagnetized they are repelled toward the exit region due to the electric potential. A maximum value of the Xe^+ density is observed at the center of the cylindrical region near the dielectric wall. From Fig. 4 we can conclude that the ionization is enhanced in this region.

The time series of the electron and Xe^+ densities averaged in the region $0 < z < 25$ mm and $0 < r < 20$

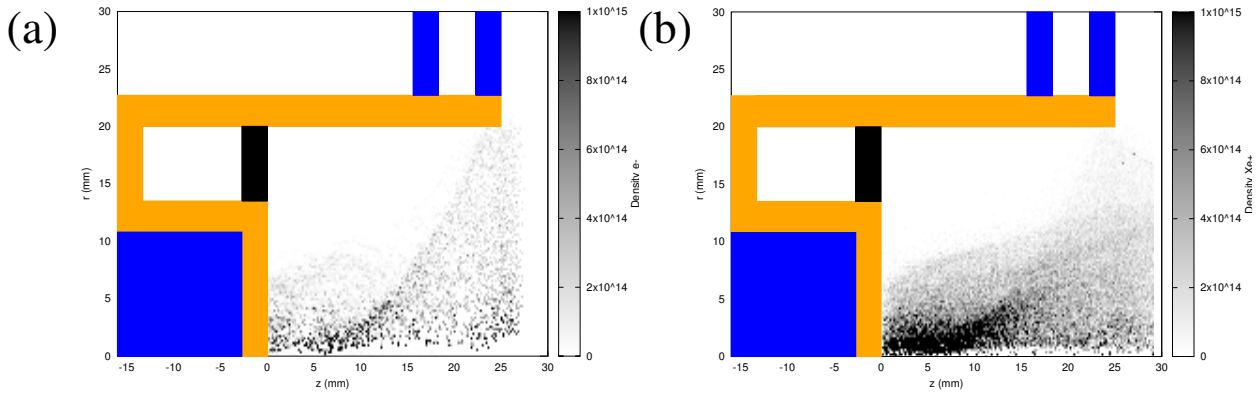

Figure 4. (a) The electron density, and (b) the ion Xe^+ density, at $t = 6.75 \times 10^{-7}$ s, represented using the gray color.

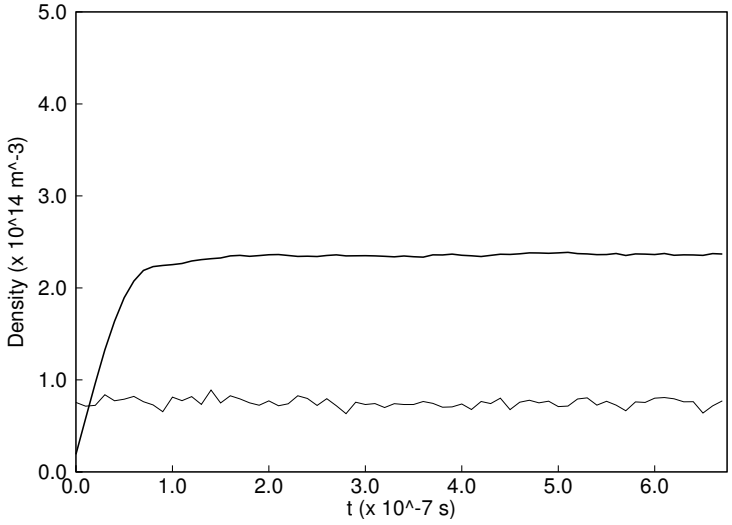

Figure 5. Time series of the average of the electron density (thin line) and time series of the average of the Xe^+ density (thick line).

mm is shown in Fig. 5. The initial transient period seen for Xe^+ is not observed in the time series of the electron density due to the higher mobility of the electron species in our simulations. The different time scales between electrons and ions also explains the presence of fluctuations in the electron density compared with the Xe^+ density in Fig. 5.

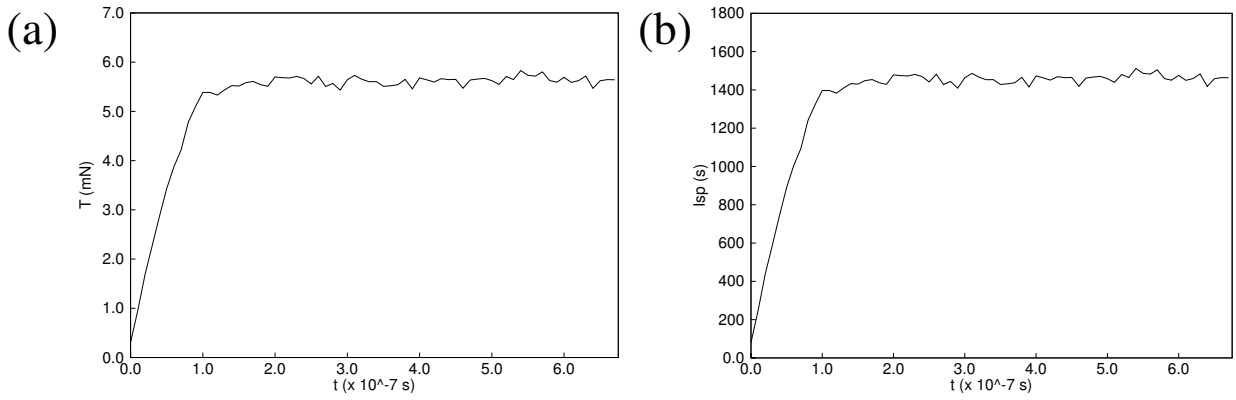

Figure 6. (a) Time series of thrust T. (b) Time series of the specific impulse I_{sp}.

Since the velocity of ions greatly exceeds the velocity of Xe neutrals in the exhaust region of conventional Hall thrusters, the thrust T can be written as[1]

$$T = \dot{m}_i \langle v_i \rangle \tag{1}$$

where $\dot{m}_i$ is the ion mass flow and $\langle v_i \rangle$ is the average ion velocity. Equation 1 can be computed from numerical simulations using the discretized form

$$T = N_p \frac{m_i}{\Delta t} \langle v_i \rangle \tag{2}$$

where N_p is the number of particles represented by a superparticle. The specific impulse I_{sp} is related to the thrust by

$$I_{sp} = \frac{T}{\dot{m} g} \tag{3}$$

where $\dot{m}$ is the Xe neutral mass flow rate, and $g = 9.8$ m/s^2 is the acceleration of gravity.

Figure 6 shows the time series of T and I_{sp} computed using Eqs. (2) and (3), respectively, from $t = 0.0$ s (i.e., when the electron source is enabled) to $t = 6.75 \times 10^{-7}$ s. There is an initial transient period until $t = 1 \times 10^{-7}$ s, after which both T and I_{sp} reach a steady state. The average value of T and I_{sp} computed during the interval $[2 \times 10^{-7}, 6.75 \times 10^{-7}]$ s gives $\langle T \rangle = 5.6 \pm 0.9$ mN, and $\langle I_{sp} \rangle = 1460.4 \pm 22.0$ s, which are close to the values reported in laboratory experiments.[10]

IV. Conclusions

In this paper we described a model of a cylindrical Hall thruster to be implemented at the Laboratory of Plasmas at the University of Brasília. The model solves the interaction of neutral and charged particles with electric and magnetic fields using a PIC technique. We applied several methods to reduce the execution time and computational effort, for example, by using superparticles[17] and geometrical scaling laws.[18] We presented results on the Xe neutrals, Xe^+ ions and electron density. We compute the thrust and the specific impulse, and our results are in agreement with laboratory experiments. The simplified model presented here will allow to explore in detail the parameter space of the CHT to find an optimal configuration.

The electron and Xe^+ densities presented in this paper show that the ionization is higher in a central region near the dielectric wall. The electron mobility in the direction perpendicular to magnetic field lines can be affected by the reduction of dimensions in 2D models. For this reason, several authors include an additional electron transport mechanism to account for this effect in numerical simulations of Hall thrusters.[19–22]

By considering an enhanced electron transport, the ionization region is higher near the anode, where the magnetic field lines accumulate.[7,11] However, the origin of this anomalous cross-field transport is not well understood.[20,23,24] Moreover, there is no general agreement on how this effect should be included in numerical simulations.[20,22,24] The inclusion of a term representing anomalous electron diffusion in our model, for example, Bohm diffusion[11] will be the focus of future work.

Acknowledgments

The authors acknowledge support from the UNIESPAÇO program of the Brazilian Space Agency (AEB), the National Council of Technological and Scientific Development (CNPq), FAPDF, IF/UnB, DPP/UnB and CAPES. R.A.M. acknowledges support from FAPDF under grant 3798.25.34800.0807/2015. A.A.M. gratefully acknowledges AEB, the National Institute for Space Research (INPE) and CNPq for the attribution of a post-doc scholarship for the development of electric propulsion systems to use in satellites.

References

[1]Goebel D M and Katz, I 2008 *Fundamentals of Electric Propulsion: Ion and Hall Thrusters* (JPL Space Sci. Tech. Series).

[2]Kim V, Kozlov V, Kazurenko A, Popov G, Skrylnikov A, Clauss C, Day M and Sankovic J 1998 *34th Joint Propulsion Conf.* (Cleveland) AIAA 98-3335.

[3]Beal B E, Gallimore, A D 2005 *Phys. Plasmas* **12** 123503.

[4]Ding Y J, Yu D R, Kia D C, Yan G J and Li H 2011 *Contrib. Plasma Phys.* **51** 68.

[5]Ahedo E and Gallardo J M 2003 *28th Intern. Electric Propulsion Conf.* (Toulouse) IEPC 2003-104.

[6]Raitses Y and Fisch N J 2001 *Phys. Plasmas* **8** 5 2579.

[7]Garrigues L, Hagelaar G J M, Boeuf J P, Raitses Y, Smirnov A and Fisch N J 2008. *IEEE Trans. Plasma Sci.* **35** 5 2008.

[8]Raitses Y, Merino E, Fisch N J 2010 *J. Appl. Phys.* **108** 093307.

[9]Smirnov A, Raitses Y, and Fisch, N J *Phys. Plasmas* **14**, 057106.

[10]Seo M, Lee J, Seon J, Lee H J and Choe, W 2013 *Phys. Plasmas* **20** 023507.

[11]Smirnov A, Raitses Y, and Fisch N J 2004 *Phys. Plasmas* **11** 4922.

[12]Matyash K, Schneider R, Kalentev O, Raitses Y and Fisch N J 2011 *The 32nd Intl. Elec. Prop. Conf.* IEPC-2011-070.

[13]Raitses Y, Smirnov A, and Fisch N J *Phys. Plasmas* **16** 057106.

[14]Ferreira J L, Martins A A, Miranda R A, Schelin A B, Alves L de S, Costa E G, Coelho E O, Serra A C B and Nathan F 2015 *J. Comp. Appl. Math* DOI 10.1007/s40314-015-0286-4.

[15]Pryor, R W 2015 *Multiphysics Modeling Using Comsol 5 and MATLAB* (Mercury Learning and Information).

[16]Choi Y, Mahalingam S, Likhanskii A. 2012 *IEEE Conf. Series* 978-1-4577-0557-1/12.

[17]Hockney R W and Eastwood J W 1988 *Computer Simulation Using Particles* (Bristol, IOP Publishing Ltd.).

[18]Taccogna F, Longo S, Capitelli M, Schneider R *Phys. Plasmas* **12** 053502.

[19]Hagelaar, G J M, Bareilles, J, Garrigues, L and Boeuf, J-P 2003 *J. Appl, Phys* **93** 67.

[20]Hagelaar, G J M 2007 *Plasma Sources Sci. Technol.* **16** S57.

[21]Hofer, R R, Katz, I, Mikellides, I G, Goebel, D M, Jameson, K K, Sullivan, R M and Johnson, L K. 2008. *AIAA/ASME/SAE/ASEE Joint Propulsion Conf. Exhib.* (Hartford), AIAA 2008-4924.

[22]Cho S, Komurasaki K, Arakawa Y 2013 *Phys. Plasmas* **20**, 063501.

[23]Boniface C, Garrigues L, Hagelaar G J M, Boeuf J P, Gawron, D and Mazouffre S 2006 *Appl. Phys. Lett.* **89**, 161503.

[24]Bultinck E, Mahieu S, Depla D, Bogaerts A 2010 *J. Phys D: Appl. Phys*, **43** 292001.